

1 **Bayesian inference of the impulse-response model of athlete training and performance**

2 Kangyi Peng^{1,2}, Ryan T. Brodie^{2,3,4}, Tim B. Swartz^{1,2}, David C. Clarke^{2,3,4,*}

3 ¹Department of Statistics and Actuarial Science, ²SFU Sports Analytics Group, ³Department of
4 Biomedical Physiology and Kinesiology, Simon Fraser University, Burnaby BC, V5A 1S6, Canada;
5 ⁴Canadian Sport Institute Pacific, Pacific Institute for Sport Excellence, 4371 Interurban Road, Victoria
6 BC, V9E 2C5 Canada.

7

8

9 *Corresponding author:

10 Email: dcclarke@sfu.ca

11 Tel: 778-782-9777

12 Fax: 778-782-3040

13

14 Running title: Bayesian inference of IR model

15 Keywords: athletic performance, mathematical modeling, Bayes Theorem, Banister impulse-response
16 model, computer simulation.

17 Word count: ~4,300

18

19 **This article is a pre-print and has not been peer reviewed.**

20

21 **Citation:** Peng, K., Brodie, R. T., Swartz, T. B., Clarke, D. C. (2023). Bayesian inference of the
22 impulse-response model of athlete training and performance. *Sportrxiv*.

23

24 **Abstract**

25 The Banister impulse-response (IR) model quantitatively relates athletic performance to training. Despite
26 its long history, the model usefulness remains limited due to difficulties in obtaining precise parameter
27 estimates and performance predictions. To address these challenges, we developed a Bayesian
28 implementation of the IR model, which formalizes the combined use of prior knowledge and data. We
29 report the following methodological contributions: 1) we reformulated the model to facilitate the
30 specification of informative priors, 2) we derived the IR model in Bayesian terms, and 3) we developed a
31 method that enabled the JAGS software to be used while enforcing parameter constraints. We applied the
32 model to the training and performance data of a national-class middle-distance runner. We specified the
33 priors from published values of IR model parameters, followed by estimating the posterior distributions
34 from the priors and the athlete's data. The Bayesian approach led to more precise and plausible parameter
35 estimates than nonlinear least squares. We then drew inferences from the Bayesian model regarding the
36 athlete's performance and showed how the method can be applied in perpetuity as new data are collected.
37 We conclude that the Bayesian implementation of the IR model overcomes the foremost challenges to its
38 usefulness for athlete monitoring.

39

40 1. Introduction

41 Maximizing athletic performance depends primarily on athletes undertaking appropriate training loads at
 42 appropriate times. Understanding the quantitative relationship between training and performance is thus
 43 of interest to athletes and their advisors. Mathematical models that predict performance from training have
 44 been proposed, with the most studied being the Banister impulse-response (IR) model (Clarke & Skiba,
 45 2013). The IR model expresses performance at time t as the sum of the initial or baseline performance
 46 capacity, P_0 , the positive training effects, and the negative training effects (Equation 1).

$$P_t = P_0 + K_1 \sum_{s=0}^{t-1} e^{-\frac{t-s}{\tau_1}} * W_s - K_2 \sum_{s=0}^{t-1} e^{-\frac{t-s}{\tau_2}} * W_s \quad (1)$$

47 K_1 and K_2 are terms that express the change in performance per unit training accomplished, τ_1 and τ_2 are
 48 constants that describe the decay rates of the positive and negative training effects over time, and W_s is
 49 the training accomplished at time = s . The model presents an intuitive framework for understanding the
 50 dynamic response to training (Clarke & Skiba, 2013). This form of the model features five adjustable
 51 parameters ($P_0, K_1, K_2, \tau_1, \tau_2$) that are typically estimated by fitting the model to data from maximal-effort
 52 performances using maximum-likelihood approaches. The model has been used to analyze and predict
 53 performance and optimize training in various sports such as cycling, running, swimming, weightlifting,
 54 and track and field events (Clarke & Skiba, 2013).

55 Despite its promise, the model features several noteworthy limitations. First, its use can be burdensome
 56 in terms of time and effort. Training load data (W_s) must be rigorously collected, which is facilitated by
 57 available wearable and portable technologies such as bicycle-mounted power meters and GPS
 58 wristwatches. High-quality performance data (P_t) must likewise be regularly collected, and this
 59 requirement particularly challenges the model's widespread use. For example, athletes may compete too
 60 infrequently to accumulate sufficient data from competitions, or they may be reluctant to devote training
 61 time to performance tests. Even if sufficient performance data are accumulated, the signal-to-noise ratio
 62 in these data is typically low for experienced athletes because their performance levels tend to be relatively
 63 stable. Accordingly, the parameters of the model are often poorly estimated (Busso & Thomas, 2006;
 64 Hellard et al., 2006). The aforementioned data challenge is difficult to overcome: IR model estimation
 65 methods employed to date are entirely data driven, with no formal way to incorporate other knowledge
 66 into the framework. Approaches to overcome these challenges are therefore sought.

67 An analogous challenge has been successfully addressed by anti-doping organizations in implementing
68 the Athlete Biological Passport (ABP). The ABP is a framework developed to monitor suspicious changes
69 in biomarkers of doping over time (Sottas, Robinson, Rabin, & Saugy, 2011). The effectiveness of the
70 ABP is challenged by the relatively infrequency of athlete testing and the measured variables being
71 influenced by both biological and nuisance technical factors. Stewards of the ABP resolved this challenge
72 in part by employing Bayesian methods, in which prior probability distributions (“priors”) based on
73 population averages define the normal ranges for the measured variables for a given athlete, and these
74 ranges are updated using data collected from the athlete (Sottas, Robinson, & Saugy, 2010). With every
75 test, the ranges become increasingly athlete specific. The ABP has been successful in reducing doping
76 prevalence. More recently, a Bayesian framework was proposed to monitor suspicious changes in
77 performance, as part of an emerging “performance passport” approach to anti-doping (Hopker et al.,
78 2020). By formalizing the judicious use of prior information, Bayesian approaches are useful when data
79 are sparse, and athletes, coaches, and sport scientists can contribute their knowledge to the specification
80 of the priors. Despite the promise of Bayesian approaches, the IR model has yet to be specified in a
81 Bayesian framework and applied in practice.

82 The purpose of this study is to cast the IR model in a Bayesian framework and to apply it to data from an
83 elite middle-distance runner. We report the following methodological contributions: first, we reformulated
84 the model to enhance our ability to specify informative prior distributions for the model parameters.
85 Second, we derived the IR model in Bayesian terms. Third, we developed a generalizable procedure for
86 imposing parameter constraints that enabled the computations to be conducted using JAGS software. We
87 then estimated the model from the runner’s data and demonstrated the superiority of Bayesian inference
88 compared to a commonly used nonlinear regression procedure in terms of the precision and plausibility
89 of the parameter estimates. We conclude that the Bayesian inference approach provides a theoretically
90 and empirically superior approach for applying the IR model to the longitudinal monitoring and prediction
91 of athletic training and performance.

92 **Methods**

93 *2.1 Study design & participant*

94 The study design was observational; we used previously collected training-load and performance data to
95 fit the models. Ethical approval was obtained from the Simon Fraser University Office of Research Ethics.
96 A Canadian national-level middle-distance runner volunteered to participate in the study and provided

97 informed consent. The athlete provided a season’s worth of training and performance data, spanning
98 September 1, 2017 to July 28, 2018 (301 days), during which time 259 workouts were documented.

99 *2.2 Training and performance data*

100 The daily training loads W_s were recorded as the individualized training impulse (TRIMPi; Manzi, Iellamo,
101 Impellizzeri, D’Ottavio, & Castagna, 2009). An athlete-specific multiplying factor was used to represent
102 the nonlinear effect of intensity on training load. The function was generated from the relationship between
103 blood lactate levels and the fraction of heart-rate reserve measured during an incremental treadmill
104 exercise test.

105 The athlete trained on 259 days during the season but TRIMPi were measured only for 173 of those days,
106 likely because the athlete did not wear the heart-rate chest strap for all workouts. We therefore imputed
107 the TRIMPi values in the following manner. First, we assumed that the TRIMPi were missing at random,
108 and we observed that they were linearly associated with the distances run (km) during the workouts
109 recorded by the GPS wristwatch. We used linear regression to quantify the relationship between TRIMPi
110 and distance run, with distance run specified as the explanatory variable and $\log(\text{TRIMPi})$ as the response
111 variable. The TRIMPi were log transformed to ensure the validity of the normality assumption of the
112 linear regression. Second, we used single imputation (Zhang, 2016), in which random errors are added to
113 the predicted values from the regression model, to ensure that the imputed values had similar variation as
114 the observed data.

115 Performance P_t was expressed as IAAF points achieved in sanctioned races. This approach was used
116 because the athletes raced over different distances (e.g., 800 m, 1,500 m, and one mile), whose times and
117 velocities are not straightforwardly comparable. Referring to equation (1), the data are denoted $P =$
118 (P_1, \dots, P_N) where N measurements were recorded.

119 *Model estimation: nonlinear least squares*

120 The parameters of the IR model (Equation 1) were estimated using nonlinear least squares. This procedure
121 finds the combination of parameter values that minimize the sum-of-squares of the residual values
122 corresponding to the modeled and measured performances (Johnson & Frasier, 1985). The method was
123 implemented in R using the “nlminb” function. Confidence intervals for the parameter values were
124 computed using a bootstrap method (Efron & Tibshirani, 1986).

125 *2.3 Model formulation*

126 We cast the IR model in a stochastic framework by reformulating the original version of the model
 127 (Equation 1) as follows:

$$P_t = P_0 + K_1 \sum_{s=0}^{t-1} e^{-\frac{t-s}{\tau_1}} * W_s - \theta * K_1 \sum_{s=0}^{t-1} e^{-\frac{t-s}{\tau_2}} * W_s + \varepsilon_t = \mu_t + \varepsilon_t \quad (2)$$

128 where μ_t is the expected value of performance, ε_t are the unobserved errors, and θ is an unknown
 129 constant greater than one that relates K_1 to K_2 . The μ_t and ε_t terms allow the model to be probabilistically
 130 assessed. In section 2.4, we discuss distributional assumptions concerning ε_t . We rewrote K_2 as $\theta * K_1$
 131 because θ is a parameter for which we have greater prior knowledge, and it is less dispersed than K_2 . The
 132 corresponding physiology imposes the restriction $\theta > 1$.

133 To enhance the interpretability of the IR model, two derived parameters are commonly calculated, t_n and
 134 t_g . t_n is the day after which training has a net negative influence on performance at time t , and t_g is the
 135 day on which training has the highest positive influence on performance at time t . t_n and t_g are computed
 136 from the following formulae:

$$t_n = \frac{\tau_1 \tau_2}{\tau_1 - \tau_2} \ln \left(\frac{K_2}{K_1} \right) \quad (3)$$

$$t_g = \frac{\tau_1 \tau_2}{\tau_1 - \tau_2} \ln \left(\frac{K_2 \tau_1}{K_1 \tau_2} \right) \quad (4)$$

137 Using these equations, θ can be rewritten entirely in terms of τ_1 , τ_2 , t_n , and t_g , which are parameters for
 138 which we have the best prior knowledge.

$$\theta = K_2/K_1 = (\tau_1/\tau_2)^{\left(\frac{1}{t_g/t_n - 1}\right)} \quad (5)$$

139 Overall, the IR model parameters $(P_0, K_1, K_2, \tau_1, \tau_2)$ are reformulated as $(P_0, K_1, \theta, \tau_1, \tau_2)$.

140 2.4 Bayesian implementation of the IR model

141 Bayesian approaches are being increasingly used in sports science and are particularly useful for
 142 applications involving elite athletes (Hecksteden et al., 2022; Santos-Fernandez, Wu, & Mengersen, 2019).
 143 Primers on the use of Bayesian approaches are available elsewhere (van de Schoot et al., 2021; Van de
 144 Schoot et al., 2014). In the Bayesian approach, a *posterior probability distribution* is obtained from the
 145 *prior distribution* and the *likelihood function*. To cast the IR model in a Bayesian framework, we first
 146 assume that the model parameters are random variables that conform to particular probability distributions.

147 The prior density $\pi(\theta)$ encodes background knowledge regarding the model parameters. The likelihood
 148 function $f(P|\theta)$ specifies the information from the data. The posterior density describes the updated
 149 probability associated with the model parameters (given the data) and is proportional to the product of the
 150 prior distribution and likelihood function, as follows:

$$\pi(\theta|P) \propto f(P|\theta)\pi(\theta) \quad (6)$$

151 where θ refers to the parameters in the IR model, including the variance parameters associated with the
 152 random error term ε_t . The vector $P = (P_1, \dots, P_N)$ is the performance data.

153 Next, we assumed that the observed performances P_1, \dots, P_N are recorded daily, although this assumption
 154 is not necessary in practice. We then assumed that the performances are correlated in time; specifically,
 155 the performance on day t is related to the performance on day $t-1, t-2$, and so on with decreasing correlation.
 156 To encode this assumption, we assumed that the error terms $\varepsilon_1, \varepsilon_2, \dots, \varepsilon_N$ conformed to the multivariate
 157 normal distribution $MVN_N(0, \Sigma)$, and we modeled the athlete's performances $[P_1, P_2, \dots,$
 158 $P_N | P_0, K_1, \theta, \tau_1, \tau_2, \Sigma]$ as $MVN_N(\mu, \Sigma)$, where $\mu = (\mu_1, \mu_2, \dots, \mu_N)$. Note that μ_t is the expected
 159 performance on day t (Equation 2). The parameter Σ is the variance-covariance matrix of the multivariate
 160 normal distribution, where the i, j^{th} term of Σ is equal to $\sigma^2 * \rho^{|i-j|}$, $0 < \rho < 1$. The parameter σ^2 is the variance
 161 term, and $\rho^{|i-j|}$ is the correlation between performances on day i and day j . When $i = j$, $\rho^{|i-j|}$ is maximized
 162 and is equal to 1; for $i \neq j$, $\rho^{|i-j|}$ decreases as $|i-j|$ increases. This stipulation reflects the notion that
 163 performances closer in time to one another are expected to be more similar. This idea has been used in the
 164 analysis of substitution times in soccer (Silva & Swartz, 2016). This parametrization is appealing due to
 165 its simplicity because the $N(N+1)/2$ parameters in Σ are reduced to two parameters (ρ, σ). Using the density
 166 function of the multivariate normal distribution, the likelihood function of the data is therefore expressed
 167 as follows:

$$f(P|\theta) = f(P|P_0, K_1, \theta, \tau_1, \tau_2, \Sigma(\sigma, \rho)) \propto \det(\Sigma(\sigma, \rho))^{-\frac{1}{2}} e^{-\frac{1}{2}(P-\mu)^T \Sigma(\sigma, \rho)^{-1} (P-\mu)} \quad (7)$$

168 **2.5 Prior elicitation**

169 The prior density $\pi(\theta)$ expresses our prior beliefs regarding the model parameters (Van de Schoot et al.,
 170 2014); it does not depend on the data. Prior elicitation involves specifying the probability distribution to
 171 which the parameter is expected to conform. The certainties of the priors are encoded in the widths of the
 172 distributions: for parameters whose values are well established, relatively strong priors are assigned,
 173 whereas the priors for parameters whose values are less certain, more diffuse priors are assigned.

174 We elicited the prior density of $\theta = (P_0, K_1, \theta, \tau_1, \tau_2, \sigma, \rho)$, which includes the five model parameters
 175 (Equation 2) and the two parameters related to the error distribution. We made the standard assumption
 176 that the priors are statistically independent. This assumption enabled us to simplify the prior density
 177 $[P_0, K_1, \theta, \tau_1, \tau_2, \sigma, \rho]$ as the product $[P_0][K_1][\theta][\tau_1][\tau_2][\sigma][\rho]$. We then assigned priors to
 178 $[P_0], [K_1], [\theta], [\tau_1], [\tau_2], [\sigma]$, and $[\rho]$. P_0 is the initial performance of the athlete and we let $[P_0] \sim \text{Normal}$
 179 (p_0, σ_{p0}) with hyper-parameters p_0 and σ_{p0} which are later specified. The parameters K_I and θ have
 180 continuous values and express the average change in IAAF scores per unit positive training effect (K_I)
 181 and per unit negative training effect ($\theta * K_I$). The specification of prior information about K_I is challenging
 182 due to the inconsistent measurements in performance and training load in different sports. Different
 183 performance and training load measurements lead to different K_I scales. We therefore assigned a flat prior
 184 with a large range to K_I as $[K_I] \sim \text{Uniform}(0, 10)$. The interpretation of θ is well understood and expressed
 185 via Equation 5. Therefore, we assigned a strong prior to θ as $[\theta] \sim \text{Normal}(4.137, 6)$, truncated $(1, \infty)$. The
 186 parameters τ_1 and τ_2 are time constants that respectively describe the temporal decays of the positive and
 187 negative training effects. Values reported in the literature spanned 4 to 169 and 1 to 69 for τ_1 and τ_2 ,
 188 respectively. Based on our experience with the model, we found these ranges to be excessively wide, such
 189 that we set the following constraints: $5 < \tau_1 < 60$ and $3 < \tau_2 < 60$. Therefore, we assigned normal
 190 priors $[\tau_1] \sim \text{Normal}(50, 38)$, truncated $(5, 60)$, and $[\tau_2] \sim \text{Normal}(13, 12)$, truncated $(3, 60)$. The parameter
 191 ρ is a correlation coefficient and $0 < \rho < 1$. The variability of ρ was assigned as $[\rho] \sim \text{Beta}(10, 1)$, where $E(\rho)$
 192 $= 0.91$. This reflects the assumption that the performance on day i and day $i - 1$ are positively correlated.
 193 For σ , we assigned the standard Jeffreys reference prior $[\sigma] \propto 1/\sigma$. And for P_0 , we assigned $[P_0] \sim \text{Normal}$
 194 $(1000, 20)$.

195 Using the likelihood function (Equation 7), the posterior density was expressed as the following product:

$$[P_0, K_1, \theta, \tau_1, \tau_2, \sigma, \rho | P] \propto f(P | \theta) [P_0] [K_1] [\theta] [\tau_1] [\tau_2] [\sigma] [\rho] \quad (8)$$

196 The specified values for the parameters and hyper-parameters are based on information from published
 197 studies featuring the IR model. Specifically, we curated studies from our personal libraries and by
 198 identifying papers that cited the original Banister et al. (1975) study and Clarke and Skiba (2013).
 199 Altogether, we compiled 40 studies, from which we extracted approximately 100 sets of estimated
 200 parameters. Of these, 57 parameter sets adhered to the assumptions of the model, which were used to
 201 inform the priors (Supplementary information <https://github.com/kenp666/IR-model>).

202 **2.6 Computation**

203 The posterior density (Equation 8) is complex and intractable, such that it is challenging to gain insights
204 into the model parameters directly. We therefore used Markov Chain Monte Carlo (MCMC) simulation
205 to generate samples of model parameters from the posterior distribution. We implemented MCMC using
206 the JAGS package in R, the code for which is provided as Supplementary Information at
207 <https://github.com/kenp666/IR-model>. A challenge with implementing MCMC is that the IR model
208 parameters have the following constraints: $0 < K_1 < K_2$, $\theta > 1$, $5 < \tau_1 < 60$, and $3 < \tau_2 < 60$, which cannot
209 be straightforwardly enforced within the JAGS software. Accordingly, an extra step in the sampling
210 procedure was introduced to implement the constraints. For each iteration in the MCMC simulation, we
211 first checked whether the constraints were satisfied. If they were satisfied, then the simulation results were
212 retained; if not, then the generated variates were discarded, and the sampling was repeated. This procedure
213 slowed the computation time, such that 1,000 iterations for adaptation and 5,000 iterations were run for
214 each model. The posterior means served as point estimates of the parameters and the lower (2.5%) and
215 upper (97.5%) quantiles of the posterior distributions served as the lower and upper bounds of the 95%
216 credible interval estimates.

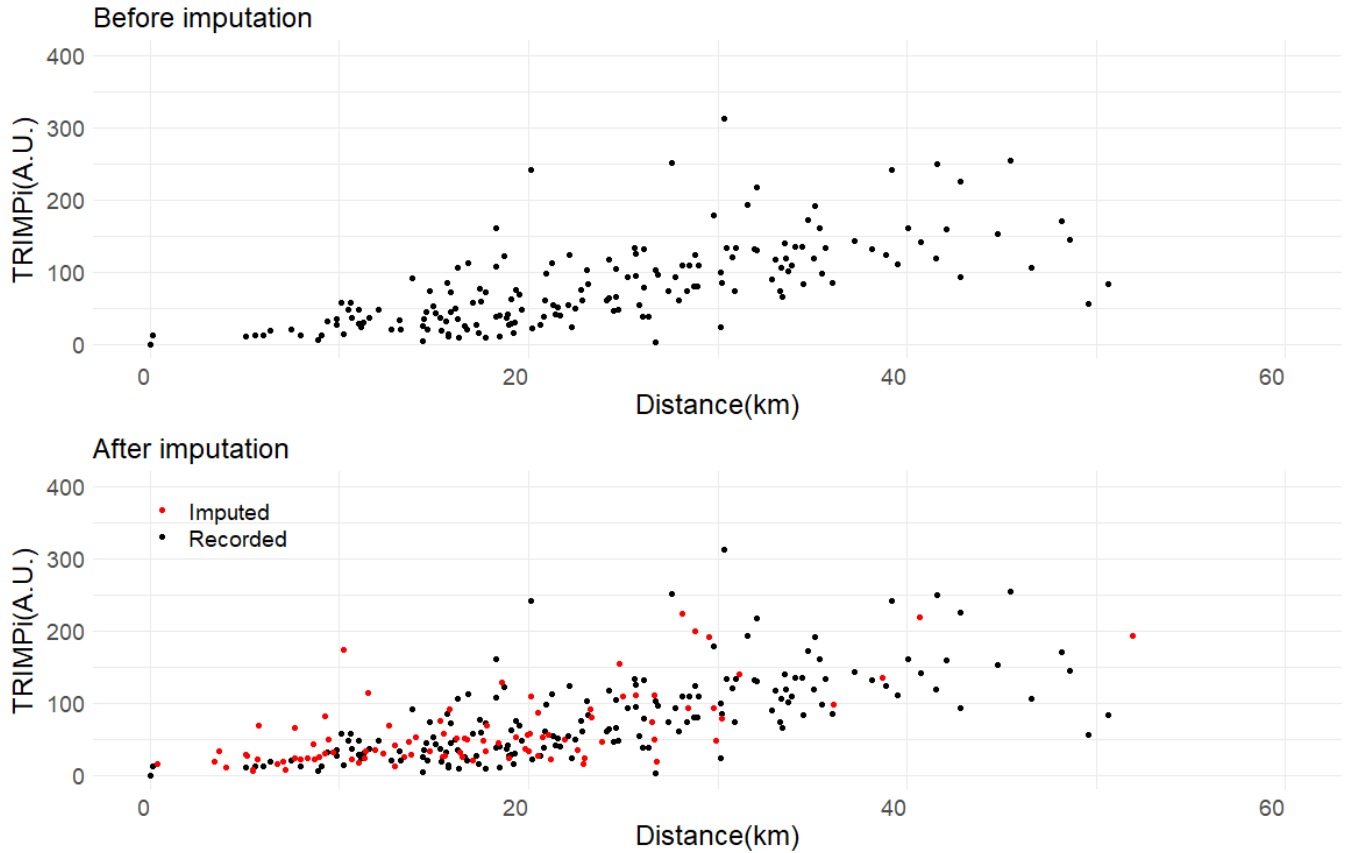
217 Predicted IAAF points, P , can also be generated from the MCMC simulations. The procedure to simulate
218 the IAAF points involved three steps (A Gelman et al., 2013). First, $(P_0, K_1, \theta, \tau_1, \tau_2, \sigma, \rho)$ are sampled
219 from the posterior distribution. Second, P is sampled from the multivariate normal distribution $[P|P_0, K_1,$
220 $\theta, \tau_1, \tau_2, \sigma, \rho]$, as expressed in Equation 6, using the sampled values of $(P_0, K_1, \theta, \tau_1, \tau_2, \sigma, \rho)$ and the
221 training loads as the inputs to the IR model. This process provided a single variate P from the predictive
222 distribution. Third, steps 1 and 2 were repeated to approximate the predictive distribution of P . The
223 prediction of P was iterated 5,000 times, resulting in a distribution of $P(t)$ trajectories. The 2.5% and 97.5%
224 quantiles were computed for $P(t)$ to estimate the 95% prediction interval of IAAF points. Standard
225 diagnostic checks were performed to assess convergence (Andrew Gelman & Rubin, 1992).

226

227 **Results**

228 *Training and performance data*

229 The runner completed 259 workouts, the distances for which were 18.7 ± 12.6 km. The athlete's distances
230 were linearly associated with the TRIMPi values ($r = 0.65$), and the missing TRIMPi were imputed as
231 described in the Methods (Figure 1).



232

233

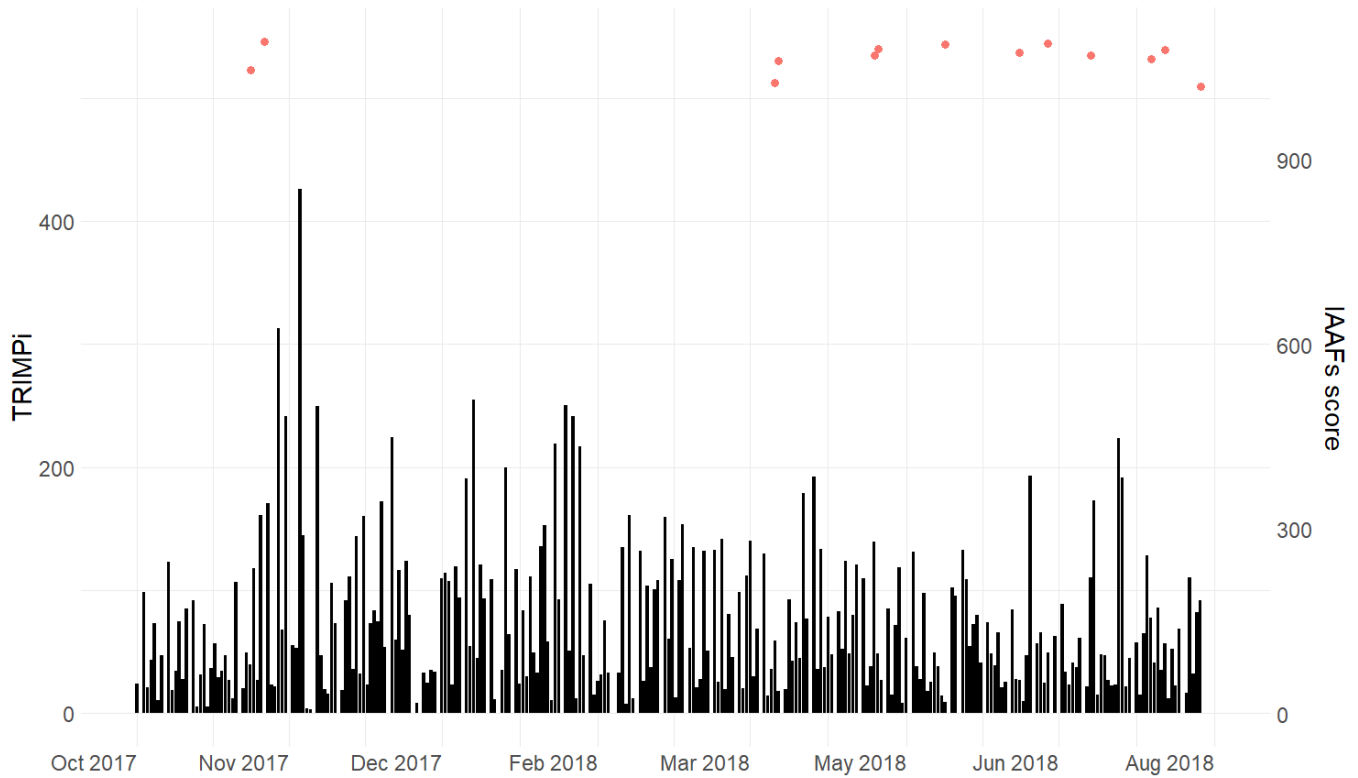
234 **Figure 1.** Scatterplots of TRIMPI_i versus distance run (km). A. Scatterplot of the measured values of
235 TRIMPI_i and workout distance (km). B. Measured values (black points) overlaid with the imputed values
236 of TRIMPI_i (red points).

237 The TRIMPI_i values (observed and imputed) are plotted by day in Figure 2. The athlete competed in 13
238 races, 10 of which were 800 m (outdoor), two were 1,500 m (outdoor), and one was 1 mile (indoor). The
239 athlete’s IAAF scores ranged from 1,018 to 1,109 points.

240

241

242



243

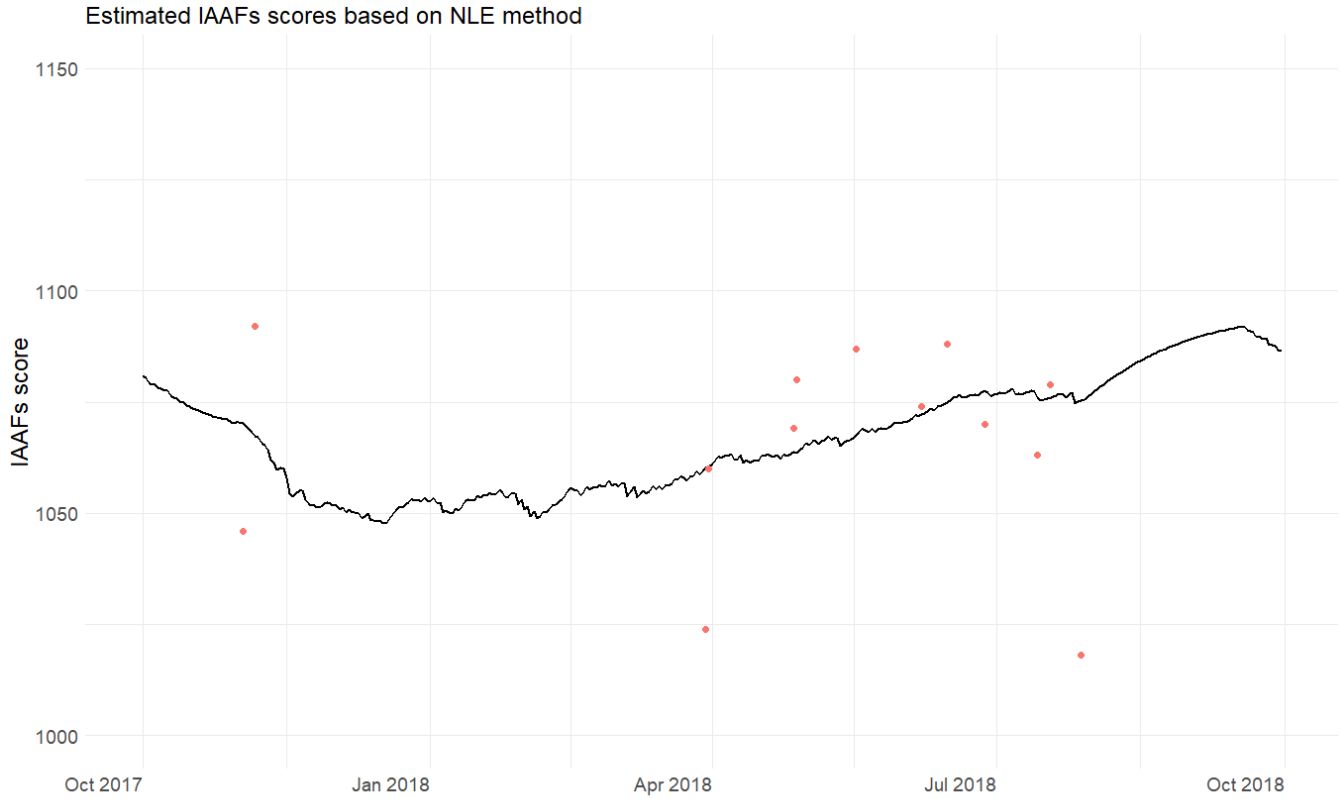
244 **Figure 2.** Training load and performances in season 2018. The black bars are the daily training loads
 245 (TRIMPi) and the red points are athlete’s performances (IAAF score) in 13 races.

246

247 *Model fitting using non-linear least squares*

248 We first fitted the IR model (Equation 1) using non-linear least squares. We observed that the model-
 249 predicted IAAF scores followed the trend of the true IAAF scores (Figure 3), and the method provided
 250 plausible estimates for P_0 , K_1 and K_2 . However, the estimated parameter values featured wide confidence
 251 intervals (Table 1). The estimated values of the well-understood parameters t_n and t_g were 84 and 155,
 252 respectively. The plausibility of these values of is questionable.

253



254

255 **Figure 3.** Modeled performance (black line) compared to performance data (IAAF scores, red points).
 256 The IR model was fitted using the non-linear least squares method.

257

258 **Table 1.** Estimated parameters and 95% confidence intervals from the nonlinear least-squares procedure.

Parameter	Estimate	95% Confidence interval
P_0	1078	1,022, 1,799
K_1	0.056	-2.82, 16.15
K_2	0.068	-2.80, 16.17
τ_1	77	-731,491, 154
τ_2	65	-5,803, 129
t_n	84	19, 617
t_g	155	-167,864, 334

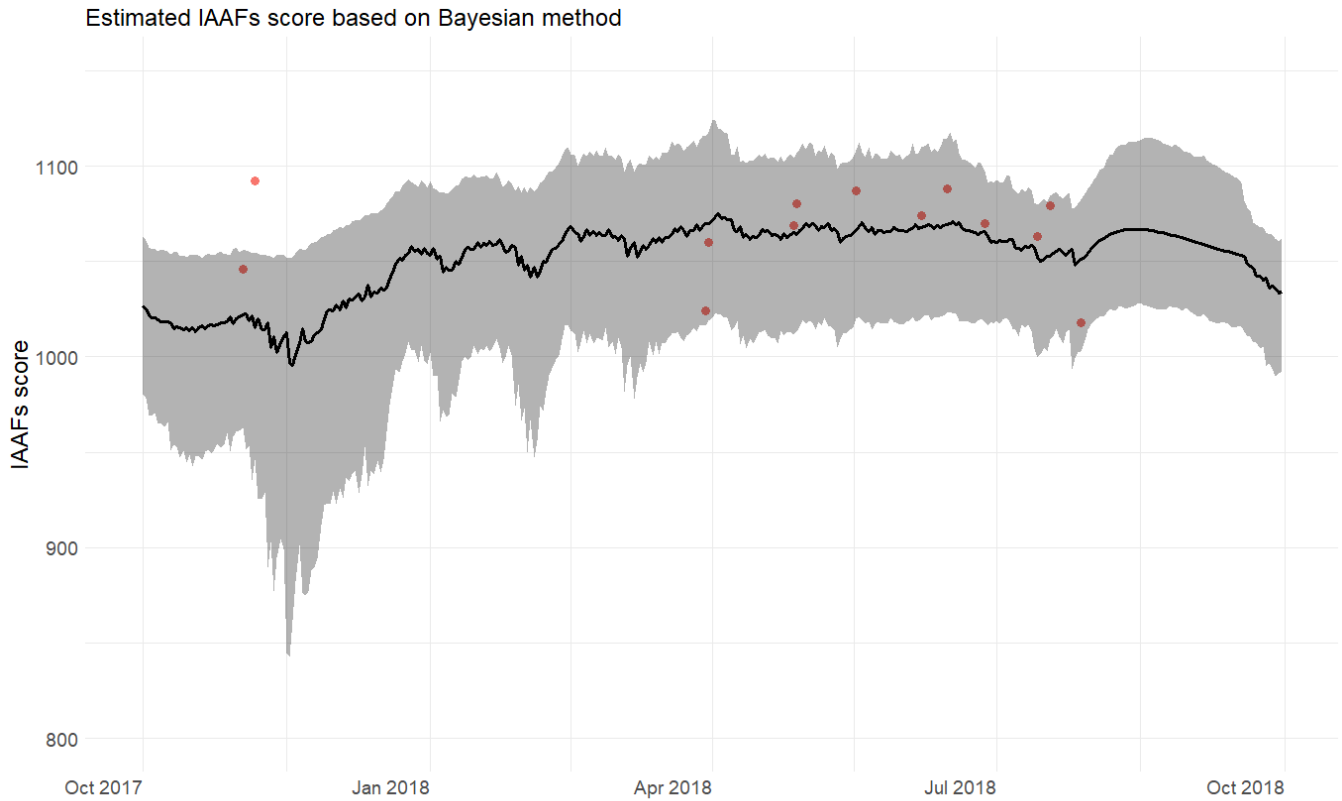
259

260 *Model fitting using the Bayesian approach*

261 The Bayesian approach led to predicted IAAF scores and corresponding 95% predictive intervals that
 262 captured most of observed IAAF scores. In addition, the fitted curve was smoother and less scattered than

263 the one from the non-linear least square estimates (Figure 4). Model diagnostics are reported in the
 264 Appendix.

265



266

267 **Figure 4.** Modeled performance (black line is the point estimates, grey shadow is the posterior predictive
 268 interval) compared to performance data (IAAF scores, red points). The IR model was fitted using Bayesian
 269 method.

270 The Bayesian approach led to parameter estimates that adhered to the IR model constraints and posterior
 271 intervals of reasonable widths (Table 2). The width of the posterior intervals of parameters t_n and t_g were
 272 still wide, but their estimates were more believable, and the fitted model can be used to suggest the taper
 273 strategy for this athlete.

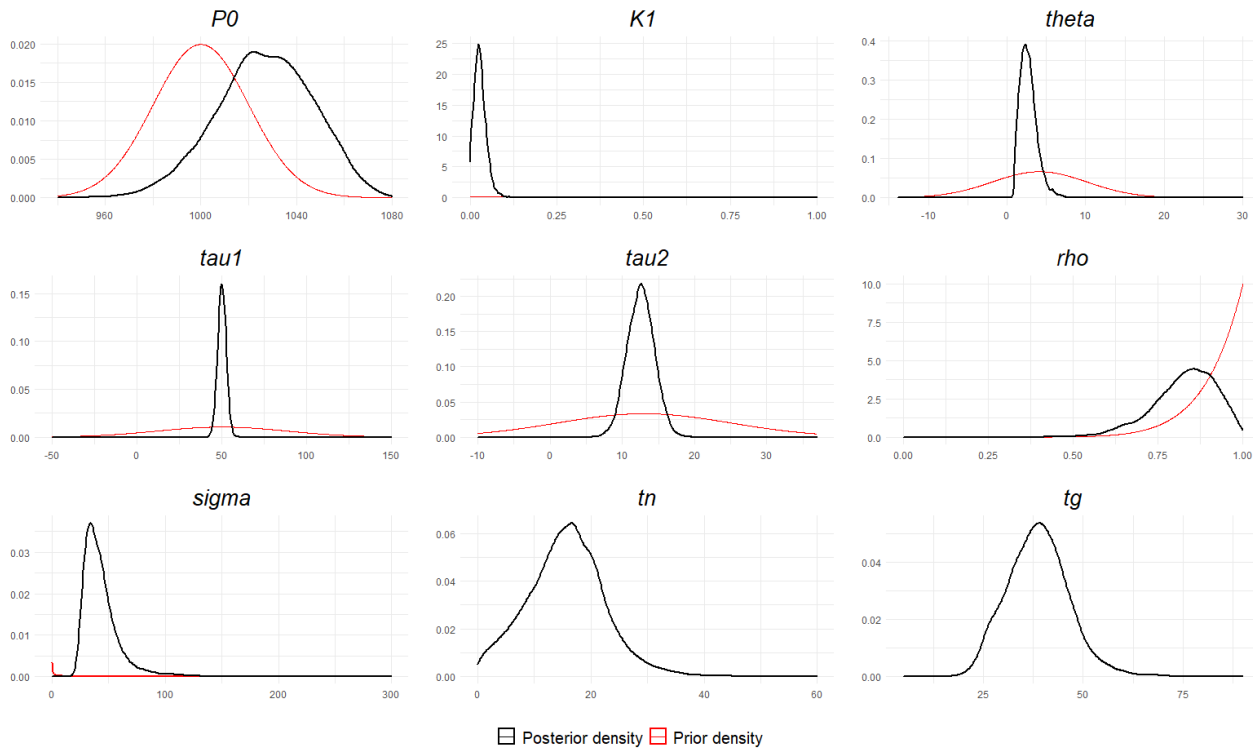
274 **Table 2.** Estimated parameters and 95% credible intervals from the Bayesian version of the IR model.

Parameter	Estimate (posterior mean)	Credible interval (2.5%, 97.5%)
P_0	1028	986, 1,063
k_1	0.028	0.0024, 0.68

θ	2.75	1.16, 5.30
τ_1	50	45, 55
τ_2	13	9, 16
t_n	16	2, 29
t_g	39	25, 55
ρ	0.83	0.61, 0.97
σ	43	25, 86

275

276 Comparing the prior and posterior distributions for parameters $P_0, K_I, \theta, \tau_1, \tau_2, \sigma$ revealed that the data
 277 had a strong influence on the posterior distributions (Figure 5). In particular, the posterior standard
 278 deviations of the parameters $\tau_1, \tau_2,$ and θ were markedly reduced, while the posterior mean of P_0 was
 279 shifted to the right. The posterior density of K_I was narrow despite its less-informative prior, which was
 280 flat and had a wide range.



281

282 **Figure 5.** Comparison of the prior (red) and posterior (black) densities for the IR model parameters.

283 **Discussion**

284 In this study, we applied Bayesian methods to the IR model involving an elite middle-distance runner. We
 285 made several methodological advances, including a reformulated the model to facilitate the specification
 286 of informative priors, we compiled published data to specify the priors, and we developed a method that

287 enabled the JAGS software to be used while enforcing logical parameter constraints. We applied the
288 Bayesian approach to the data from a national-class middle-distance runner, and compared the fits to those
289 obtained using nonlinear least squares. Our proof-of-principle results demonstrate that the Bayesian
290 approach method is superior to nonlinear least squares because the estimated parameter values from the
291 former were more precise, well behaved, and believable. Bayesian inference led to actionable insights
292 whereas the nonlinear least squares approach did not.

293 Bayesian methods offer theoretical and practical advantages compared to frequentist methods such as
294 nonlinear least squares, and are finding increasing use in the sport science literature (Hecksteden et al.,
295 2022; Hopker et al., 2020). First, the nonlinear least squares approach relies solely on the data for fitting
296 models, such that the procedure will work poorly when the data are sparse, the results are highly sensitive
297 to noise. The present data set featured relatively few performances, because middle-distance runners tend
298 to compete sporadically, and there was considerable variability in the data that could have unduly
299 influenced the model fit. Bayesian methods, by contrast, can still be used when data are sparse and can be
300 more robust to noise depending on the strengths of the priors. A second advantage of Bayesian methods
301 is the ability to iterate the procedure as new data become available, which is particularly useful for
302 longitudinal athlete monitoring. In this case, the posterior distribution from the 2018 season could be
303 specified as the prior distribution for the following season. Specifically, the results from Table 2 would
304 be used to specify the priors as follows: $[K_I] \sim \text{Normal}(0.038, 0.02)$; $[\theta] \sim \text{Normal}(\mu_\theta = 2.78, \sigma_\theta = 1.1)$,
305 $\text{truncated}(1, \infty)$; $[\tau_1] \sim \text{Normal}(\mu_{\tau_1} = 49, \sigma_{\tau_1} = 2.6)$, $\text{truncated}(5, 60)$; $[\tau_2] \sim \text{Normal}(\mu_{\tau_2} = 13, \sigma_{\tau_2} = 1.9)$,
306 $\text{truncated}(3, 60)$; $[P_0] \sim \text{Normal}(p_0 = 1025, \sigma_{p_0} = 20)$; $[\sigma^2] \propto \text{inverse gamma}(0.001, 0.001)$; and $[\rho] \sim \text{Beta}$
307 $(10, 1)$. Note that the P_0 of the following season is the predicted performance from the end of the 2018
308 season, and the prior for K_I is specified as a normal distribution. In addition, the widths of the new priors
309 are less than those of the 2018 season and are therefore more informative.

310 The results of the analysis can be interpreted to provide practical interpretations and advice for the athlete,
311 from both retrospective and predictive standpoints. From a retrospective standpoint, the predicted
312 performance from the Bayesian model demonstrated that the athlete improved in the early part of the
313 season, from December to April, and then maintained their performance level during the competition
314 period (April to July). Such a pattern might be expected if the athlete is competing frequently and has less
315 opportunity for high volumes of training. For this athlete, the training loads during the competition phase
316 may have been insufficient to support an increase in performance in the latter part of the season. From a

317 predictive standpoint, the estimated t_g of 39 days suggests that training quantity and quality should be
318 maximized approximately 40 days before the main competition, which could inform the scheduling of
319 future training camps. The estimated t_n of 16 days suggests that the athlete would most benefit from tapers
320 lasting approximately 2.5 to 3 weeks. The Bayesian model could be used to predict the effects of different
321 training programs simulated as TRIMPi profiles over time (Clarke & Skiba, 2013).

322 While the Bayesian approach addresses some of the foremost challenges limiting the usefulness of the IR
323 model, particularly those relevant to parameter estimation, it does not overcome all of them. For example,
324 owing to diffuse priors and sparse few data, the prediction intervals may be overly wide for some
325 applications. While the Bayesian approach may be less sensitive to noise in the data, the quality of training
326 and performance data still matters. Here our data set featured missing training data, which we addressed
327 using imputation, but it would have been preferable if we had more complete training data. We also
328 quantified performance using IAAF points, because this metric enables races of different distances to be
329 used as performance data. However, IAAF points for middle-distance races are a function of race time
330 and placing, and such races are not always run as well-paced maximal efforts. Race tactics, such as a
331 conservatively paced first half, can confound the performance data. Further research is needed to propose
332 and evaluate improved performance metrics. Finally, the Bayesian approach does not overcome the
333 theoretical shortcomings of the IR model, such as the assumption that performance is solely a function of
334 training load. That said, the Bayesian approach is general and can be applied to future improved versions
335 of the IR model.

336 In summary, we have developed here a Bayesian implementation of the Banister IR model. We made
337 several methodological contributions and showed proof-of-principle by applying the approach to analyze
338 the training and performance data from a national-class middle-distance runner. The Bayesian approach
339 outperformed nonlinear least squares and provided actionable insights for the athlete. The Bayesian
340 implementation of the IR model helps to overcome several of the IR model's foremost challenges that
341 have heretofore impaired its practical usefulness.

342 **Acknowledgements**

343 This study was funded by an Own The Podium-Mitacs Accelerate Fellowship to RTB and DCC and by a
344 Canadian Statistical Sciences Institute Collaborative Research Team grant in sports analytics. TBS and
345 DCC are supported by grants from the Natural Sciences and Engineering Research Council of Canada.

346 The authors thank Dr. Marc D. Klimstra of the Canadian Sport Institute Pacific and University of Victoria
347 for his support and guidance. The authors have no conflicts of interest to disclose.

348 **References**

- 349 Banister, E. W., Calvert, T. W., Savage, M. V., & Bach, T. (1975). A Systems Model of training for
350 athletic performance. *Australian Journal of Sports Medicine*, 7, 57–61.
- 351 Busso, T., & Thomas, L. (2006). Using mathematical modeling in training planning. *International Journal*
352 *of Sports Physiology and Performance*, 1(4), 400–405.
- 353 Clarke, D. C., & Skiba, P. F. (2013). Rationale and resources for teaching the mathematical modeling of
354 athletic training and performance. *Advances in Physiology Education*, 37(2), 134–152.
355 <https://doi.org/10.1152/advan.00078.2011>
- 356 Efron, B., & Tibshirani, R. (1986). Bootstrap methods for standard errors, confidence intervals, and other
357 measures of statistical accuracy. *Statistical Science*, 54–75.
- 358 Gelman, A, Carlin, J. B., Stern, H. S., Dunson, D. B., Vehtari, A., & Rubin, D. B. (2013). *Bayesian data*
359 *analysis* (3rd ed.). Boca Raton, FL: CRC Press.
- 360 Gelman, Andrew, & Rubin, D. B. (1992). Inference from iterative simulation using multiple sequences.
361 *Statistical Science*, 457–472.
- 362 Hecksteden, A., Forster, S., Egger, F., Buder, F., Kellner, R., & Meyer, T. (2022). Dwarfs on the Shoulders
363 of Giants: Bayesian Analysis With Informative Priors in Elite Sports Research and Decision Making.
364 *Frontiers in Sports and Active Living*, 4.
- 365 Hellard, P., Avalos, M., Lacoste, L., Barale, F., Chatard, J. C., & Millet, G. P. (2006). Assessing the
366 limitations of the Banister model in monitoring training. *J Sports Sci*, 24(5), 509–520.
- 367 Hopker, J., Griffin, J., Brookhouse, J., Peters, J., Schumacher, Y. O., & Iljukov, S. (2020). Performance
368 profiling as an intelligence-led approach to antidoping in sports. *Drug Testing and Analysis*, 12(3),
369 402–409.
- 370 Johnson, M. L., & Frasier, S. G. (1985). [16] Nonlinear least-squares analysis. In *Methods in enzymology*
371 (Vol. 117, pp. 301–342). Elsevier.
- 372 Manzi, V., Iellamo, F., Impellizzeri, F., D'Ottavio, S., & Castagna, C. (2009). Relation between
373 Individualized Training Impulses and Performance in Distance Runners. *MEDICINE AND SCIENCE*

- 374 *IN SPORTS AND EXERCISE*, 41(11), 2090–2096. <https://doi.org/10.1249/MSS.0b013e3181a6a959>
- 375 Santos-Fernandez, E., Wu, P., & Mengersen, K. L. (2019). Bayesian statistics meets sports: a
376 comprehensive review. *Journal of Quantitative Analysis in Sports*, 15(4), 289–312.
- 377 Silva, R. M., & Swartz, T. B. (2016). Analysis of substitution times in soccer. *Journal of Quantitative*
378 *Analysis in Sports*, 12(3), 113–122.
- 379 Sottas, P.-E., Robinson, N., Rabin, O., & Saugy, M. (2011). The athlete biological passport. *Clinical*
380 *Chemistry*, 57(7), 969–976.
- 381 Sottas, P.-E., Robinson, N., & Saugy, M. (2010). The Athlete’s Biological Passport and Indirect Markers
382 of Blood Doping. In *Doping in sports: Biochemical principles, effects and analysis. Handbook of*
383 *Experimental Pharmacology*, vol 195. (pp. 305–326). Berlin, Heidelberg: Springer.
384 https://doi.org/10.1007/978-3-540-79088-4_14
- 385 van de Schoot, R., Depaoli, S., King, R., Kramer, B., Märtens, K., Tadesse, M. G., ... others. (2021).
386 Bayesian statistics and modelling. *Nature Reviews Methods Primers*, 1(1), 1–26.
- 387 Van de Schoot, R., Kaplan, D., Denissen, J., Asendorpf, J. B., Neyer, F. J., Van Aken, M. A. G., ... Van
388 Aken, M. A. G. (2014). A gentle introduction to Bayesian analysis: Applications to developmental
389 research. *Child Development*, 85(3), 842–860.
- 390 Zhang, Z. (2016). Missing data imputation: focusing on single imputation. *Annals of Translational*
391 *Medicine*, 4(1).

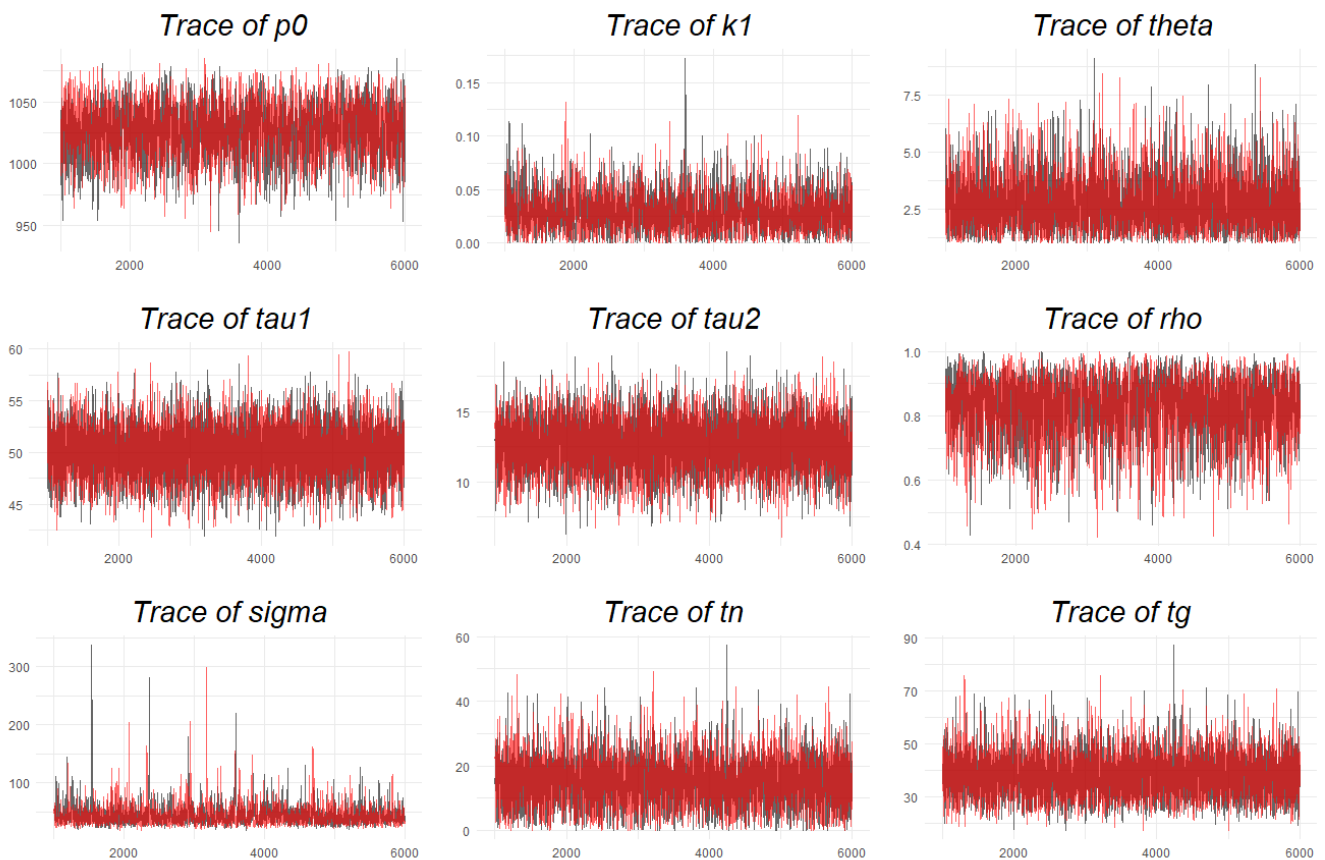
392

393

394 **Appendix**

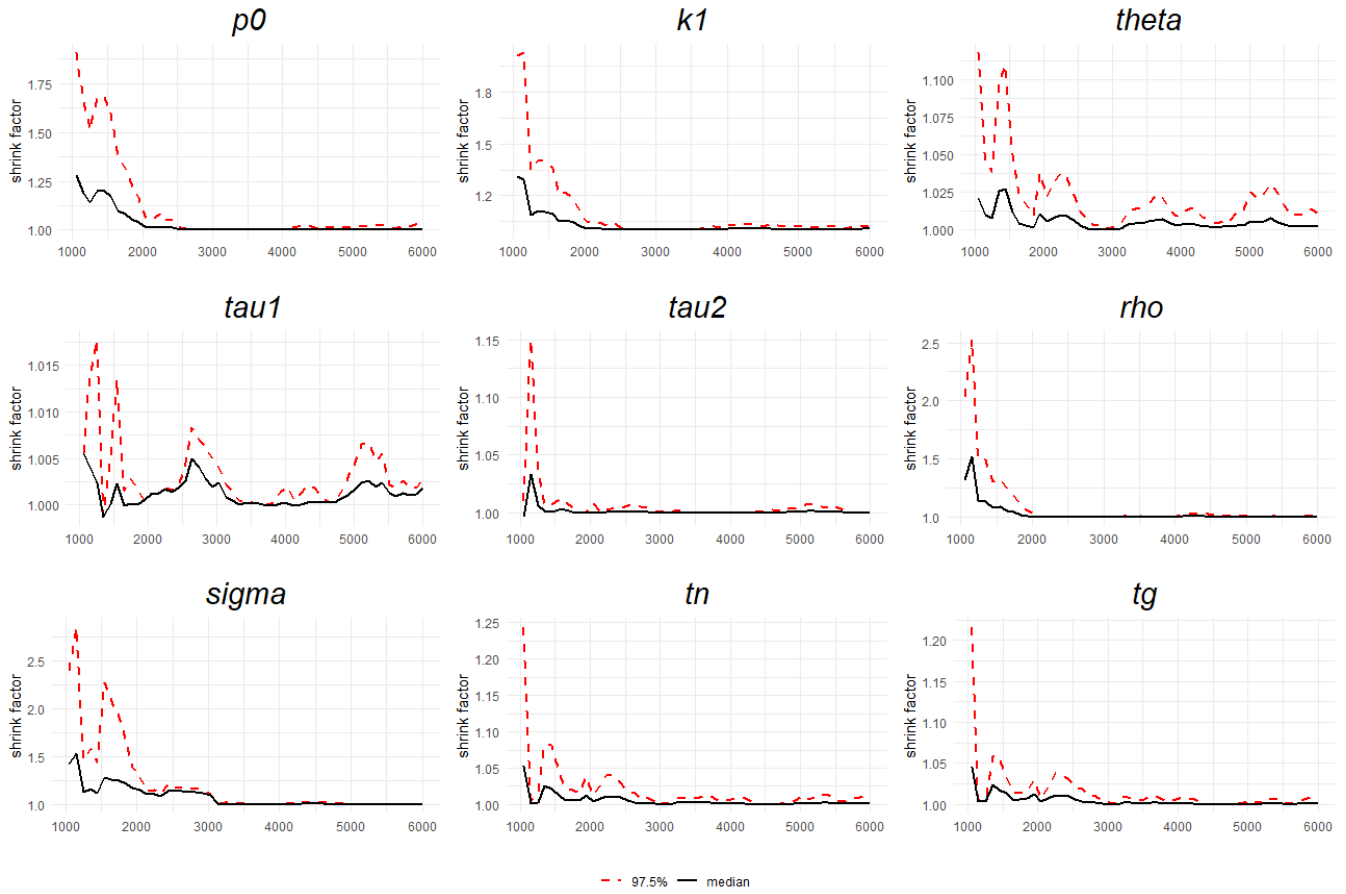
395 *Bayesian model diagnostics*

396 We checked the convergence of MCMC simulation with trace plots (Figure A1). The plot shows that the
 397 two chains (black and red) rapidly converged in the first few iterations, and both chains converged to
 398 similar estimates. The Gelman Rubin Diagnostic (\hat{R} , “shrink factor”) value were low for each parameter,
 399 and they approached values equal to 1 within approximately 2,000 iterations, which further indicated that
 400 the MCMC converged (Figure A2). Therefore, we used the first 2,000 iterations as the “burn in” and
 401 retained the last 3,000 iterations as our sample of the posterior.



402

403 **Figure A1.** IR model parameter diagnostics. The x-axes of the plots are the iteration number, while the y-
 404 axes are the values of the indicated IR model parameter. Each plot includes trace plots for two chains,
 405 indicated by the red and black lines.



406

407 **Figure A2.** IR model diagnostics. Gelman Rubin Diagnostic (\hat{R} , y-axis) are plotted as a function of the
408 iteration number (x-axis). The red dashed line represents the upper bound of \hat{R} (97.5% quantile) and the
409 black solid line represents the point estimates for \hat{R} . \hat{R} values equal to ~ 1 imply that the MCMC algorithm
410 converged.

411